THE JOURNAL OF BIOLOGICAL CHEMISTRY VOL. 286, NO. 4, pp. 2719–2727, January 28, 2011
Printed in the U.S.A.

LPS Impairs Phospholipid Synthesis by Triggering β-Transducin Repeat-containing Protein (β-TrCP)-mediated Polyubiquitination and Degradation of the Surfactant Enzyme Acyl-CoA:Lysophosphatidylcholine Acyltransferase I (LPCAT1)*

Received for publication, October 7, 2010, and in revised form, November 9, 2010 Published, JBC Papers in Press, November 11, 2010, DOI 10.1074/jbc.M110.192377

Chunbin Zou[‡], Phillip L. Butler[‡], Tiffany A. Coon[‡], Rebecca M. Smith[‡], Gary Hammen[§], Yutong Zhao[‡], Bill B. Chen[‡], and Rama K. Mallampalli[‡¶‖1]

From the [‡]Department of Medicine, Acute Lung Injury Center of Excellence, University of Pittsburgh, Pittsburgh, Pennsylvania 15213, the [¶]Medical Specialty Service Line, Veterans Affairs Pittsburgh Healthcare System, Pittsburgh, Pennsylvania 15240, the [‖]Department of Cell Biology and Physiology, University of Pittsburgh, Pittsburgh, Pennsylvania 15260, and the [§]Department of Anatomy and Neurobiology, Washington University, St. Louis, Missouri 63110

Acyl-CoA:lysophosphatidylcholine acyltransferase 1 (LPCAT1) is a relatively newly described and yet indispensable enzyme needed for generation of the bioactive surfactant phospholipid, dipalmitoylphosphatidylcholine (DPPtdCho). Here, we show that lipopolysaccharide (LPS) causes LPCAT1 degradation using the Skp1-Cullin-F-box ubiquitin E3 ligase component, β-transducin repeat-containing protein (β-TrCP), that polyubiquitinates LPCAT1, thereby targeting the enzyme for proteasomal degradation. LPCAT1 was identified as a phosphoenzyme as Ser^{178} within a phosphodegron was identified as a putative molecular recognition site for glycogen synthase kinase-3β (GSK-3β) phosphorylation that recruits β-TrCP docking within the enzyme. β-TrCP ubiquitinates LPCAT1 at an acceptor site (Lys^{221}), as substitution of Lys^{221} with Arg abrogated LPCAT1 polyubiquitination. LPS profoundly reduced immunoreactive LPCAT1 levels and impaired lung surfactant mechanics, effects that were overcome by siRNA to β-TrCP and GSK-3β or LPCAT1 gene transfer, respectively. Thus, LPS appears to destabilize the LPCAT1 protein by GSK-3β-mediated phosphorylation within a canonical phosphodegron for β-TrCP docking and site-specific ubiquitination. LPCAT1 is the first lipogenic substrate for β-TrCP, and the results suggest that modulation of the GSK-3β-$SCF\beta^{TrCP}$ E3 ligase effector pathway might be a unique strategy to optimize dipalmitoylphosphatidylcholine levels in sepsis.

Phosphatidylcholine (PtdCho)[2] is the predominant component of pulmonary surfactant and of eukaryotic cellular membranes. The major surface-active form of lipid within the lung surfactant is dipalmitoylphosphatidylcholine (DPPtdCho), which is produced both by *de novo* synthesis and by remodeling within lung alveolar epithelial type II cells. It is estimated that over half of DPPtdCho within the surfactant is generated from the remodeling pathway (1–3). In this pathway, 1-palmitoyl, 2-unsaturated fatty acid PtdCho is hydrolyzed by a phospholipase A_2-generating lysophosphatidylcholine (lyso-PtdCho) that subsequently is reacylated to DPPtdCho using palmitate as a substrate. Until recently, the identity of this acyltransferase was unknown. The enzyme that catalyzes the acyltransferase reaction was recently cloned from lung epithelia, has a highly conserved HX_4D motif necessary for catalytic activity typical of homologous acyltransferases, and is termed acyl-CoA:lysophosphatidylcholine acyltransferase (LPCAT1) (4, 5). Importantly, LPCAT1 is abundant in lung type II cells and exhibits substrate selectivity for palmitate suggesting that it may be critical for maintaining DPPtdCho production in a salvage pathway or to complement *de novo* synthesis of surfactant during inflammatory stress (4, 5). LPCAT1 activity increases with lung development and in response to glucocorticoids, perhaps secondary to increased LPCAT1 gene transcription (4). Indeed, mice harboring a hypomorphic allele of LPCAT1 succumb to perinatal death from reduced surfactant (6). LPCAT1 tightly maintains surfactant balance in cells by regulating *de novo* synthesis of PtdCho (7). The data thus far underscore the potentially critical role of this enzyme biologically, and yet limited data are available on its molecular control.

The ubiquitin-proteasomal machinery degrades the majority of proteins in mammalian cells. The conjugation of ubiquitin to a target protein is orchestrated by a series of enzymatic reactions involving an E1 ubiquitin-activating enzyme, ubiquitin transfer from an E1-activating enzyme to an E2-conjugating enzyme, and last, generation of an isopeptide bond between the substrate's ϵ-amino lysine and the C terminus of ubiquitin catalyzed by a E3-ubiquitin ligase. Monoubiquitinated or multiubiquitinated proteins may be processed within the lysosomal/endocytic pathway, whereas polyubiquitinated proteins are commonly targeted for 26 S proteaso-

* This work was supported, in whole or in part, by National Institutes of Health Grants HL096376, HL097376, and HL098174 (to R. K. M.) and RO1 HL091916 (to Y. Z.). This work was also supported by a Merit Review Award from the United States Department of Veterans Affairs.

[1] To whom correspondence should be addressed: Dept. of Medicine, Division of Pulmonary, Allergy, and Critical Care Medicine, 628 NW Montefiore, 3459 Fifth Ave., Pittsburgh, PA 15213. Tel.: 412-692-2112; Fax: 412-692-2260; E-mail: mallampallirk@upmc.edu.

[2] The abbreviations used are: PtdCho, phosphatidylcholine; DPPtdCho, dipalmitoylphosphatidylcholine; MLE, murine lung epithelial cells; β-TrCP, β-transducin repeat-containing protein; SCF, Skp1-Cullin-F-box; oligo, oligonucleotide.

mal degradation (8). There exist two major classes of ubiquitin ligases as follows: the RING finger (cullin containing) and the HECT domain ligases (9). The Skp1-Cullin1-F-box protein (SCF) complex is a well characterized RING finger E3-ubiquitin ligase implicated in the regulation of cell death, proliferation, and survival. The SCF machinery contains a receptor component, F-box, that confers substrate specificity for the complex (9). Of over 60 F-box proteins that have been described to date, β-transducin repeat-containing protein (β-TrCP) is one F-box subunit within SCF complexes ($SCF^{\beta\text{-}TrCP}$) that has emerged as a critical regulator of cyclin-dependent kinases and gene transcription (10). The $SCF^{\beta\text{-}TrCP}$ ubiquitin ligase catalyzes ubiquitination of its targets by recognizing specific molecular signatures (DSG*XX*S destruction motif) within substrates, whereby Ser is first phosphorylated, that then facilitates β-TrCP docking. Thus, kinase-specific phosphorylation is an important post-translational event within target substrates prior to $SCF^{\beta\text{-}TrCP}$-driven substrate ubiquitination and proteolytic processing.

Glycogen synthase kinase 3β (GSK-3β) has emerged as a key regulatory enzyme that phosphorylates numerous substrates linked to diverse cellular processes. In the lung, GSK-3β regulates the inflammatory immune response, the cell cycle, and apoptotic program (11, 12). GSK-3 is constitutively active in cells, is inhibited by upstream signals (*e.g.* PI3K-Akt pathway), and regulates the stability of increasing numbers of protein substrates (13). For example, in the case of β-catenin, GSK-3-driven phosphorylation of specific residues ((S/T)*XXX*(S/Tp) is the GSK-3 consensus phosphorylation signature) within this substrate facilitates binding of β-TrCP, to allow its subsequent ubiquitination and degradation. In general, the second (C-terminal) serine or threonine is usually primed by phosphorylation by a second kinase before GSK-3 phosphorylates the N-terminal sites. Likewise, GSK-3β mediates phosphorylation and subsequent degradation of the sterol regulatory element-binding protein family of transcription factors involved in cholesterol metabolism. Here, a phosphodegron within SREBP1a serves as a recognition motif for the SCF^{Fbw7} ubiquitin ligase to enhance its ubiquitination and degradation after site-specific phosphorylation mediated by GSK-3 (14). Sterol regulatory element-binding proteins, to date, however, represent the only lipogenic target for SCF ubiquitin ligases.

In this study, we demonstrate that LPCAT1 is phosphorylated by GSK-3β that subsequently signals its polyubiquitination by β-TrCP and proteolysis within the 26 S proteasome. We have identified putative GSK-3β phosphorylation sites, a molecular signature for β-TrCP docking, and a polyubiquitination acceptor site within the enzyme. We observe that these molecular sites and their effectors, GSK-3β and β-TrCP, are physiologically relevant with regard to LPCAT1 processing in the context of a sepsis-induced acute lung injury model. The data provide the first evidence that a lipid-metabolizing protein is a target for $SCF^{\beta\text{-}TrCP}$ ubiquitin ligase that could impact surfactant homeostasis during inflammatory injury.

EXPERIMENTAL PROCEDURES

Cells and Reagents—Murine lung epithelial (MLE) cells were maintained with HITES medium complemented by 10% FBS in a 37 °C incubator with a supplement of 5% CO_2. Rabbit LPCAT1 polyclonal antibody was generated by Covance (Princeton, NJ). V5 antibody, mammalian expression plasmid pcDNA3.1/HisV5-topo, and *Escherichia coli* Top10 competent cells were purchased from Invitrogen. Wild type, hyperactive, or kinase-dead GSK-3β plasmids were generous gifts from Dr. John Engelhardt (15). The HA-ubiquitin construct was a generous gift from Dr. Peter M. Snyder. Phosphoserine antibodies were from Cell Signaling (Danvers, MA). The siRNAs and GSK-3, mouse V5 monoclonal, and phosphoGSK-3 antibodies were from Santa Cruz Biotechnology (Santa Cruz, CA). Immobilized protein A/G beads were obtained from Pierce. Proteasome inhibitor MG132 was from Calbiochem. HA antibody, leupeptin, cycloheximide, *E. coli* lipopolysaccharide (LPS), and phosphatase inhibitor mixtures were from Sigma. Gel extraction kits and QIAprep spin miniprep kits were from Qiagen (Valencia, CA). All materials in highest grades used in the experiments are commercially available.

Plasmid Construction and Expression—Full-length mouse *Lpcat1* cDNA was amplified by PCR using forward primer 5′-CACCATGAGGCTGCGGGGCCGCGGGCCG-3′ and reverse primer 5′-GTCCGCTTTCTTACAAGAATTCTT-TCTCCCAAAG-3′ and *Lpcat1* ORF (Open Biosystems) as a template. The PCR product was cloned into the pcDNA3.1/His/V5 vector, and the accuracy of the cDNA sequence was confirmed by DNA sequencing. Site-directed mutagenesis was performed by using the QuikChange site-directed mutagenesis kit (Stratagene, La Jolla, CA) following the directions of manufacturer using pcDNA3.1/hisV5/*Lpcat1* plasmid as a template and appropriate primers (16). Individual SCF F-box subunits were cloned as described previously (17). Cells were nucleofected with plasmids as described previously (16). Briefly, 1 million MLE cells in their exponential growth stage were suspended in 100 μl of nucleofection buffer (20 mM of Hepes in PBS buffer) and well mixed with 3 μg of plasmid DNA in an electroporation cuvette. Electroporation was performed with pre-set program T-013 in Nucleofection™ II system (Amaxa Biosystems, Gaithersburg, MD), and the cells were cultured in 2 ml of complete HITES medium for 18 h. siRNA oligos were also delivered into cells by using nucleofection with the same protocol, and 0.5 μM siRNA oligos was used in each nucleofection (16).

LPCAT1 Activity—Cells were harvested in lysis buffer (250 mM sucrose, 10 mM Tris-HCl, pH 7.4), and equal amounts of microsomal cellular protein or cell lysate were used in the assay. One nmol of 1-palmitoyl-*sn*-glycero-3-phosphocholine was added for every microliter of 5× assay buffer (final working concentration 65 mM Tris-HCl, pH 7.4, 10 mM $MgCl_2$, 12.5 mM fatty acid-free BSA, 2 mM EDTA) and sonicated. 35 μl of H_2O and cellular protein (10 μg) was added to 10 μl of sonicated assay buffer containing 5 μl of [1-^{14}C]acyl-CoA (0.1 μCi, 1.8 nmol) for a total assay volume of 50 μl. Upon addition of [1-^{14}C]acyl-CoA, samples were incubated at 30 °C for

10 min, after which the reaction was terminated by addition of chloroform/methanol/H_2O (1:2:0.70, v/v). Total cellular lipids from reaction mixtures were extracted by the method of Bligh and Dyer and spotted on LK5D plates, and PtdCho was resolved using TLC and detected using a Bioscan AR-2000 scintillation plate reader (7).

Immunoprecipitation and Immunoblot Analysis—Cell lysates were prepared by brief sonication of harvested cells in Buffer A (150 mM NaCl, 50 mM Tris-HCl, 1 mM EDTA, 2 mM dithiothreitol, 0.025% of sodium azide, 1 mM phenylmethylsulfonyl fluoride, 1% of Triton X-100, and appropriate amounts of protease inhibitor mixture, pH 7.4). For immunoprecipitation, 1 ml of cleared cell lysates (contains 1 mg of protein) were incubated with 5 μg of specified antibody at 4 °C for overnight rotation, and 20 μl of protein-AG-agarose beads were added in and mixed by rotation for another 2 h. Agarose beads were then collected and washed three times by using 1 ml of Buffer A, and the precipitates were separated by SDS-PAGE and subjected to immunoblotting analysis. Immunoblotting was performed as described, and images were obtained with Carestream Kodak *in vivo* Image F Pro System. Antibodies were diluted as 1:1000 except when specifically indicated.

In Vitro Ubiquitin Conjugation Assay—^{35}S-Labeled substrate LPCAT1 was synthesized using TnT cell-free reticulocyte lysate *in vitro* transcription/translation system with pcDNA3.1/His/V5/*Lpcat1* as template (Promega). SCF-box protein Skp1, Cullin1, Rbx1, and substrate-specific E3 ubiquitin ligase subunit, β-TrCP, were expressed in mammalian HEK293 cells and purified with Ni^{2+} beads. The ubiquitination assay was performed in a total volume of 25 μl containing 50 mM Tris, pH 7.6, 5 mM $MgCl_2$, 0.6 mM DTT, 2 mM ATP, 1.5 ng/μl E1 (Boston Biochem), 10 ng/μl Ubc5, 10 ng/μl Ubc7, 1 μg/μl ubiquitin (Calbiochem), 1 μM ubiquitin aldehyde, 2 μl of each His-purified recombinant Cullin1, Skp1, Rbx1, and β-TrCP at room temperature for 30 min. Reaction mixtures were then resolved on SDS-PAGE, followed by transferring to a nitrocellulose membrane and autoradiography.

Fluorescence Microscopy—PCR-based strategies were used to create compatible restriction enzyme sites that would allow construction of chimeric cDNAs for microscopy as described previously (28). *Lpcat1* and *β-TrCP* were amplified using PCR prior to cloning into pAmCyan-C1 or pZsYellow1-C1 (Clontech), generating *Lpcat1-CFP* or β-TrCP-YFP, respectively. For analysis of LPCAT1 and β-TrCP localization, cells were first plated at 0.12×10^6 cells/well in a two-chamber cover glass system and co-transfected with *Lpcat1-CFP* and *β-TrCP-YFP* (2 μg of plasmid/chamber) with FuGENE 6 (6 μl). LPCAT1 and β-TrCP were detected at the single cell level using a combination laser-scanning microscope system (Nikon A1; Nikon, Japan). To achieve excitation, the 458- and 514-nm line of an argon ion laser was focused through the ×60 oil differential interference contrast objective lens onto the cell. Emissions of YFP and cyan fluorescent proteins were collected through 535–595- and 470–500-nm barrier filters, respectively. The results were analyzed through Nikon NIS-Elements software.

In Vitro GSK-3β Kinase Phosphorylation Assay—V5-tagged wild type LPCAT1 and S178A, S182A, and S178A/S182A mutated LPCAT1s were expressed in cells and lysed in Buffer A with sonication. The cleared cell lysates were incubated with LPCAT1 antibody overnight and protein A/G-agarose beads for 2 h with rotation at 4 °C. The beads were washed three times with 1 ml of GSK-3β kinase assay buffer (25 mM MOPS, 12.5 mM β-glycerol phosphate, 25 mM $MgCl_2$, 5 mM EGTA, 2 mM EDTA, 0.25 mM DTT, pH 7.2). *In vitro* phosphorylation reactions were conducted by combining 40 μl of protein A/G-agarose bead- bonded LPCAT1 and 10 μl of kinase assay buffer containing 1 μCi of [γ-^{32}P]ATP and 0.1 μg of active GSK-3β (per each reaction) for 30 min at room temperature. Active GSK-3β was denatured at 95 °C for 10 min as the kinase negative control. The reactions were terminated by addition of SDS loading buffer, and the samples were separated by SDS-PAGE, and phosphorylated LPCAT1 was visualized by autoradiography.

Animals—Lenti-*Lpcat1* viral and control constructs were generated by the virus core at the University of Iowa. C57BL/6J mice were administered intratracheal lenti-empty or lenti-*Lpcat1* (10^8 plaque-forming units/mouse) for 96 h prior to intratracheal inoculation with LPS (5 mg/kg) for 24 h. Animals were then mechanically ventilated, and lung resistance, compliance, and elastance (lung stiffness) were measured, and pressure-volume loops were generated. Each group contained 5–9 mice. Lung tissues from mice were homogenized and sonicated in cell lysis buffer followed by immunoblotting analysis. All procedures were executed in accordance with approved protocols through the University of Pittsburgh Institutional Animal Care and Use Committee.

Statistical Analysis—Statistical analysis was carried out by two-way analysis of variance. Data are presented as mean ± S.D.

RESULTS

LPCAT1 Is Degraded by Ubiquitin-Proteasome—In the process of investigating regulation of proteolytically sensitive enzymes involved in PtdCho biosynthesis (7), we tested the stability of the LPCAT1 protein. MLE cells in their exponential growth phase were treated with 10 μg/ml cycloheximide, and LPCAT1 mass was analyzed over time (Fig. 1*A*). The results indicated that endogenous LPCAT1 $t_{½}$ is ~4.5 h (Fig. 1*B*). These results were consistent with $t_{½}$ of overexpressed LPCAT1 using similar methods (Fig. 1*C*). Two major routes for elimination of proteins include the proteasome and/or lysosome. In cells treated with the proteasomal inhibitor MG132 (20 μM), LPCAT1 levels were remarkably stabilized with accumulation by 24 h (Fig. 1, *D* and *E*). In contrast, in cells exposed to a lysosomal inhibitor, leupeptin, LPCAT1 mass remained unchanged overall (Fig. 1*F*). We next assessed if LPCAT1 is modified by ubiquitination as a sorting signal for proteasomal targeting. In the presence of ubiquitin aldehyde (which inhibits deubiquitination activity) and MG132, we detected a robust polyubiquitinated LPCAT1 signal in cell lysates (Fig. 1*G*). Furthermore, cells were co-transfected with V5-tagged LPCAT1 and HA-tagged ubiquitin plasmids, and lysates were subjected to HA-tagged immunoprecipitation

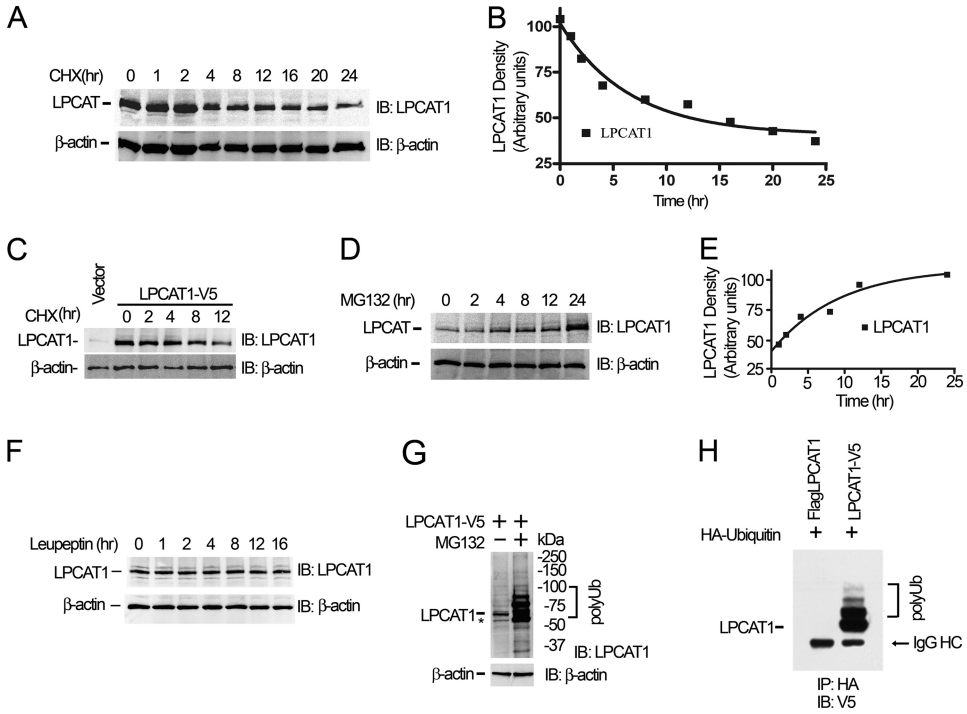

FIGURE 1. **LPCAT1 is degraded by the ubiquitin-proteasomal pathway.** *A,* MLE cells during exponential growth were serum-starved and treated with 10 μg/ml cycloheximide (*CHX*) in a time course. Cells were lysed and subjected to LPCAT1 and β-actin immunoblotting (*IB*). *B,* densitometry results of the immunoblotting were plotted for half-life analyses using PRISM software. *C,* LPCAT1 was overexpressed in cells for 18 h, and cells were treated and analyzed as in *A*. *D–F,* cells were serum-starved and treated with MG132 (20 μg/ml) (*D* and *E*) or leupeptin (20 μg/ml) (*F*) in a time course and analyzed by LPCAT1 and β-actin immunoblotting. Data in *E* show levels of LPCAT1 accumulation over time. *G,* V5-LPCAT1 was overexpressed in cells prior to treatment with or without MG132 (20 μg/ml) for 24 h. Cells were lysed in the presence of 1 μg/ml ubiquitin aldehyde and subjected to LPCAT1 immunoblot analyses. *Asterisk* represents endogenous LPCAT1. Multiple polyubiquitin (*polyUb*) bands were detected. *H,* HA-tagged ubiquitin and FLAG or V5-tagged LPCAT1 were co-expressed in cells. Cell lysates were immunoprecipitated (*IP*) with HA antibody, and the precipitates were analyzed by V5 immunoblotting. Each panel is representative of three to six independent experiments, with the exception of *E* and *F* ($n = 1$).

and probed with V5-antibody. Here, V5-LPCAT1 was also polyubiquitinated (Fig. 1*H*). These results indicate that both endogenous and overexpressed LPCAT1 are degraded by the ubiquitin proteasome machinery but not within the lysosome in epithelia.

SCF$^{\beta\text{-}TrCP}$ Triggers LPCAT1 Ubiquitination—Data base analysis identified that LPCAT1 harbors several candidate phosphorylation sites, and the enzyme was effectively phosphorylated *in vitro* (see below). As SCF E3 ligases often target phosphoenzymes for ubiquitination, we performed an unbiased screen analyzing several candidate SCF F-box components on their ability to degrade LPCAT1. Of the candidate F-box proteins expressed in epithelia, only β-TrCP reproducibly produced LPCAT1 degradation (Fig. 2*A*). Co-expression of β-TrCP with LPCAT1 in cells led to a marked reduction in immunoreactive basal levels of the enzyme (Fig. 2*B*). β-TrCP expression also reduced LPCAT1 activity by ~90% under these conditions (Fig. 2*C*). E3 ubiquitin ligases specifically bind to their targets to provide a niche for the E2 ubiquitin conjugation enzyme to catalyze the covalent ligation between ubiquitin and the acceptor lysine residues of the targeted protein. Consistent with this mechanism, co-immunoprecipitation studies demonstrated that endogenous LPCAT1 binds to β-TrCP (Fig. 2*D*). We tested *in vitro* ubiquitinating activity of β-TrCP by incubating LPCAT1 with Skp1, Cullin1, E2 conjugation enzyme-binding protein Rbx1, and ubiquitin. As shown in Fig. 2*E* (*left panel*), each SCF subunit in the ubiquitin conjugation reaction was sufficiently expressed. Here, ubiquitin was conjugated into LPCAT1 substrate with the appearance of multiple slower migrating bands suggestive of polyubiquitinated products. Levels of LPCAT1 were markedly reduced in cells exposed to cycloheximide. However, when cells were exposed to β-TrCP siRNA compared with scrambled RNA, enzyme levels recovered significantly (Fig. 2*F*). These results demonstrate that β-TrCP is an essential E3 SCF component that regulates stability and enzymatic behavior of LPCAT1.

The minimal consensus recognition sequence for β-TrCP binding within targets is S*XXX*S. Sequence alignment with lysophospholipid acyltransferases uncovered that this motif is well conserved within LPCAT1 (Fig. 3*A*). To test whether this motif is an authentic β-TrCP-binding site, we generated constructs where we substituted Ser^{178} and/or Ser^{182} with Ala in the motif. MLE cells were nucleofected with wild type pcDNA3.1/*Lpcat1* or serine-mutated LPCAT1 containing plasmids and treated with MG132 for 16 h. Robust accumulation of LPCAT1 in the presence of MG132 was observed in wild type (WT) LPCAT1 plasmid nucleofected cells but not in cells expressing S178A, S182A, or S178A/S182A mutant constructs (Fig. 3*B*). These results were confirmed in cells treated over time with the proteasomal inhibitor where again WT LPCAT1 accumulation was detected, but the LPCAT1 variants showed limited, if any, accumulation (Fig. 3*C*). In studies where V5-LPCAT1 was immunoprecipitated and products immunoblotted with β-TrCP antibody, β-TrCP bound wild

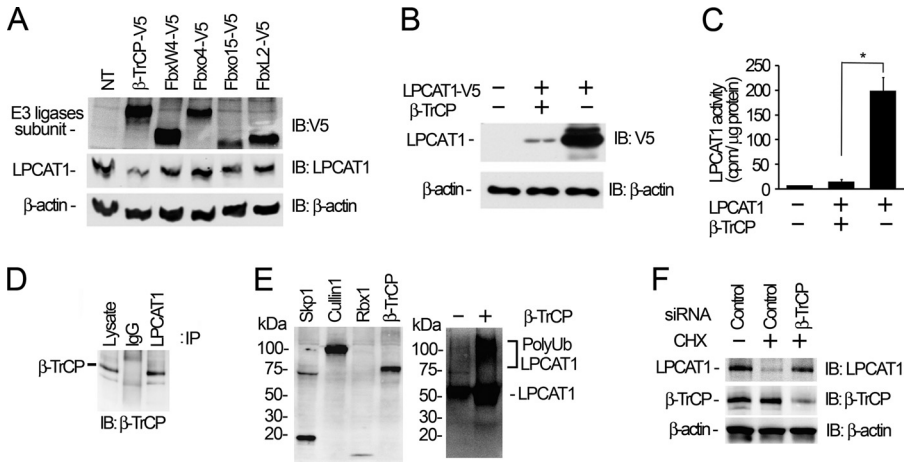

FIGURE 2. **SCF$^{\beta\text{-TrCP}}$ ubiquitinates LPCAT1.** *A,* MLE cells were cultured alone (nontransfected cells (*NT*)) or overexpressed with candidate V5-tagged SCF E3 ubiquitin ligase subunits. Cell lysates were subjected to V5, LPCAT1, and β-actin immunoblotting (*IB*). *B,* cells were nucleofected with pcDNA3.1/*His/V5/Lpcat1* plasmid or co-nucleofected with pcDNA3.1/*His/V5/β-TrCP* plasmids for 18 h. Cell lysates were subjected to V5 immunoblotting (*B*) or LPCAT1 activity (*C*) analysis. *, $p < 0.05$ by analysis of variance. *D,* cell lysates were immunoprecipitated (*IP*) (10% input) with LPCAT1 antibody and the precipitates analyzed by β-TrCP immunoblotting. *E, in vitro* ubiquitination assays were conducted ("Experimental Procedures."). *Left panel* shows the input of SCF-box subunit protein components, and *right panel* shows ubiquitination reactions using these components in the presence (+) or absence (−) of β-TrCP in the reaction mixtures. Products were run on SDS-PAGE and immunoblotted using LPCAT1 antibody. The bands below ~45 kDa represent non-specific proteins. *F,* β-TrCP-specific siRNA oligos were nucleofected in MLE cells for 48 h. Cells were treated with 10 μg/ml cycloheximide for times as indicated. Cell lysates were subjected to immunoblotting. Each panel is representative of three independent experiments, with the exception of *E* ($n = 2$). *PolyUb,* polyubiquitin.

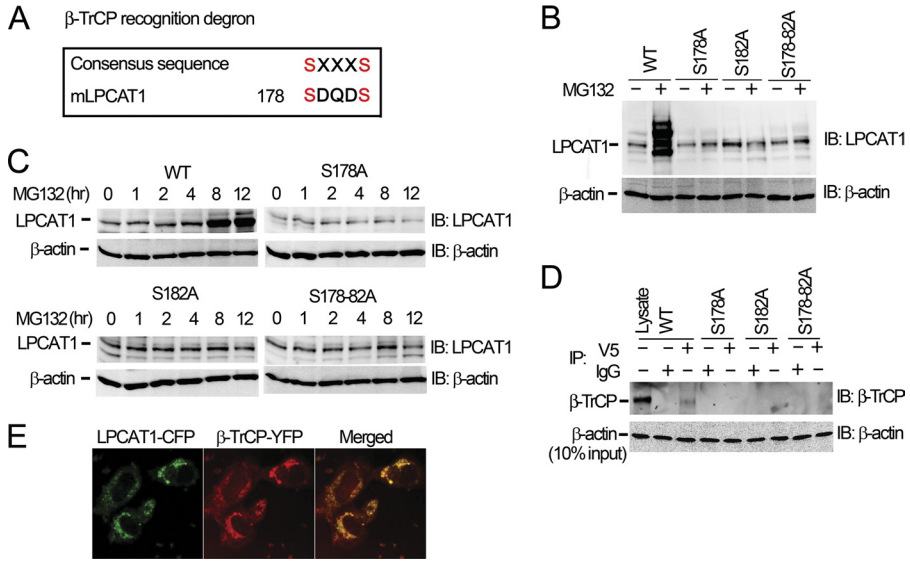

FIGURE 3. **A conserved β-TrCP-docking site resides in LPCAT1.** *A,* alignment of the amino acid sequence of a putative β-TrCP recognition degron within LPCAT1 and the known consensus sequence. *B,* MLE cells were nucleofected with wild type (*WT*) and serine-mutated LPCAT1 plasmids, respectively, for 24 h in the presence or absence of MG132. Cell lysates were analyzed by LPCAT1 immunoblotting (*IB*). Plasmids encode WT, and two point mutants (S178A and S182A) and a double mutant S178A/S182A within LPCAT1. *C,* cells were nucleofected with wild type or individual serine-mutated LPCAT1 plasmids. Nucleofected cells were treated with MG132 in a time course analysis, and cell lysates were subjected to LPCAT1 immunoblotting. *D,* wild type or serine-mutated LPCAT1 were overexpressed in cells. Cell lysates were subjected to V5 antibody immunoprecipitation (*IP*) followed by β-TrCP immunoblotting. Each panel is representative of three independent experiments. *E,* co-localization of LPCAT1 and β-TrCP. Cells were co-transfected with LPCAT1-CFP and β-TrCP-YFP (2 μg of plasmid/chamber), and LPCAT1 and β-TrCP localization was detected at the single cell level using a combination laser-scanning microscope system.

type LPCAT1, but not the Ser LPCAT1 mutants (Fig. 3*D*). These results identify that Ser^{178} and Ser^{182} are indispensable for β-TrCP docking and subsequent ubiquitination within LPCAT1. Finally, cells transfected with LPCAT1-CFP or β-TrCP-YFP were visualized by confocal microscopy demonstrating co-localization of proteins within the cytoplasm (Fig. 3*E*).

GSK-3β Phosphorylates LPCAT1—We hypothesized that serine residues in the β-TrCP-docking motif within LPCAT1 might include a GSK-3β-phosphorylated signature for E3 ligase recognition. To verify this hypothesis, we silenced the GSK-3β gene and assessed LPCAT1 degradation. GSK-3β was knocked down by siRNA, and levels were reduced further in the presence of cycloheximide (Fig. 4*A*). As before, cycloheximide effectively reduced LPCAT1 levels, an effect reversed using GSK-3β siRNA but not control RNA oligos (Fig. 4*A*). We next co-overexpressed wild type, hyperactive, or kinase-dead GSK-3β plasmids with either WT LPCAT1 or Ser-mutated LPCAT1 plasmids in cells. Expression of kinase-dead GSK-3β or wild type GSK-3β produced no effect or only min-

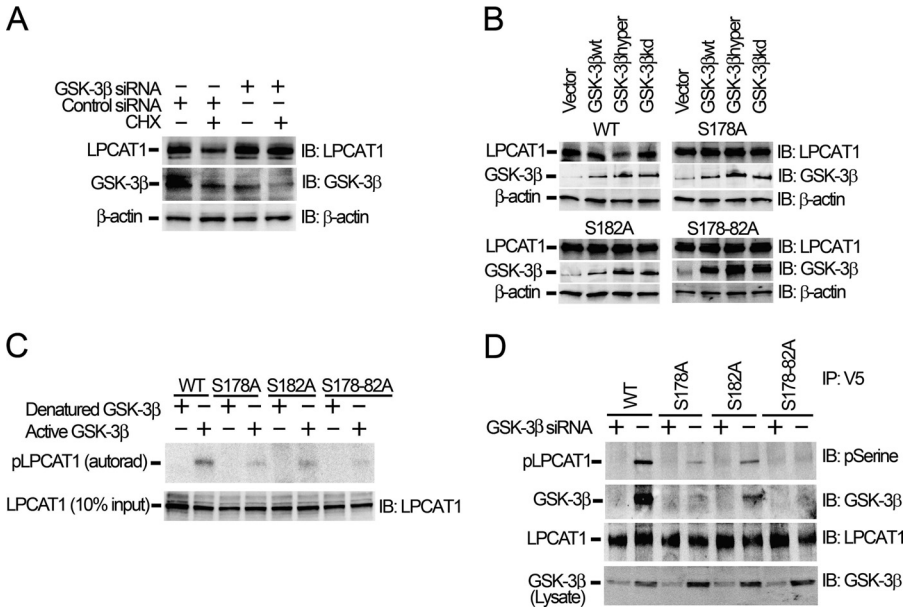

FIGURE 4. **GSK-3β phosphorylates LPCAT1.** *A,* MLE cells were nucleofected with GSK-3β-specific siRNA or control RNA oligos followed by cycloheximide (*CHX*) treatment. Cell lysates were subjected to LPCAT1, GSK-3β, and β-actin immunoblotting (*IB*). *B,* wild type (GSK-3βwt), hyperactive (GSK-3βhyper), and kinase-dead (GSK-3βkd) GSK-3β plasmids and wild type or serine-mutated LPCAT1 plasmids were co-nucleofected in MLE cells for 16 h. Cell lysates were analyzed by immunoblotting as indicated. *C,* LPCAT1 *in vitro* phosphorylation assays were performed (see under "Experimental Procedures"). V5-tagged wild type and serine-mutated LPCAT1 were overexpressed in cells, and LPCAT1 was isolated with LPCAT1 antibody and protein A/G-agarose beads. *Lower panel* shows the input of LPCAT1 that was visualized by V5 immunoblotting. *D,* V5-tagged wild type and Ser^{178} and/or Ser^{182}-mutated LPCAT1 plasmids were co-overexpressed with or without GSK-3β siRNA in MLE cells, and cell lysates were subjected to V5 immunoprecipitation followed by immunoblotting using phosphoserine antibodies to detect phosphorylated LPACT1 (*pLPCAT1*). Immunoblots were also probed with antibodies for LPCAT1 and GSK-3β. Cell lysates (10% input) were used for immunoblotting analyses as indicated. *A* and *D* are representative of five and three independent experiments, respectively, and the other panels are duplicate experiments.

imally reduced LPCAT1 levels, respectively; expression of hyperactive GSK-3β significantly reduced LPCAT1 protein (Fig. 4*B*). Levels of the LPCAT1 Ser mutants were not affected by co-expression of any of the three GSK-3β plasmids indicating that these phosphorylation residues (S178A and S182A) are relevant for LPCAT1 destabilization. As a more direct approach, *in vitro* phosphorylation assays were conducted using immunoprecipitated LPCAT1 and Ser mutants as substrates using ^{32}P-labeled ATP (Fig. 4*C*). WT LPCAT1 was phosphorylated by active but not denatured GSK-3β; phosphorylation of LPCAT1 variants harboring point mutations (S178A or S182A) was reduced, and phosphorylation of the doubly mutated protein (S178A/S182A) was drastically decreased. To assess LPCAT1 phosphorylation in cells, we overexpressed V5-tagged WT and mutated LPCAT1 plasmids in cells and silenced GSK-3β prior to V5 immunoprecipitation and by probing with phosphoserine antibody (Fig. 4*D*). Serine residues within WT LPCAT1 were robustly phosphorylated; however, knockdown of GSK-3β completely nullified its phosphorylation. In preparations isolated from cells expressing LPCAT1 S178A or S182A plasmids, detectable phosphorylation was reduced. Signal intensity of the S178A mutant was less than the S182A variant, and only a trace phosphorylation signal was detected in the LPCAT1 Ser double mutant (Fig. 4*D*). Interestingly, when we probed V5 antibody immunoprecipitates with GSK-3β, the kinase directly associated with wild type LPCAT1, but this interaction was again reduced greater in the S178A mutant *versus* the S182A variant (Fig. 4*D*, *2nd row*). Taken together, these observations suggest that specific molecular sites appear to be phosphorylated by GSK-3β, which in turn signals binding interactions between the acyltransferase and the E3 ligase subunit to regulate LPCAT1 stability in cells.

Lys^{221} Is a Bona Fide Site for LPCAT1 Ubiquitination—To identify putative ubiquitin acceptor sites within LPCAT1, we substituted several candidate Lys residues with Arg within the functional domains that were predicted to be cytosolically exposed and did not reside within the N-terminal transmembrane region of the enzyme. These constructs were expressed in cells, and LPCAT1 accumulation was measured in the presence of proteasomal blockade. Of several mutants tested, only a K221R LPCAT1 mutant was not observed to be polyubiquitinated in the presence of MG132. As a representative immunoblot, Fig. 5*A* shows that the K221R mutant, unlike WT LPCAT1, K191R, or K199R mutants, remained relatively unmodified in the presence of MG132 (Fig. 5*A*). These observations were confirmed in kinetic studies where by 8–12 h all the constructs exhibited increasing intensities of native and upper bands with the exception of the K221R mutant (Fig. 5*B*). Densitometric analysis of immunoblots is shown in Fig. 5*C* revealing a ~2-fold increase in levels of WT LPCAT1, K191R, or K199R mutants *versus* the K221R mutant. Finally, we co-expressed WT LPCAT1 and Lys mutant plasmids together with HA-tagged ubiquitin (Fig. 5*D*). Ubiquitinated proteins were immunoprecipitated with an HA antibody, and immunoblotting was performed on the precipitates using a V5 antibody. As showed in Fig. 5*D*, wild type and K199R mutated LPCAT1 were ubiquitinated in a similar manner, but the K221R mutant LPCAT1 was not ubiquitinated. Thus,

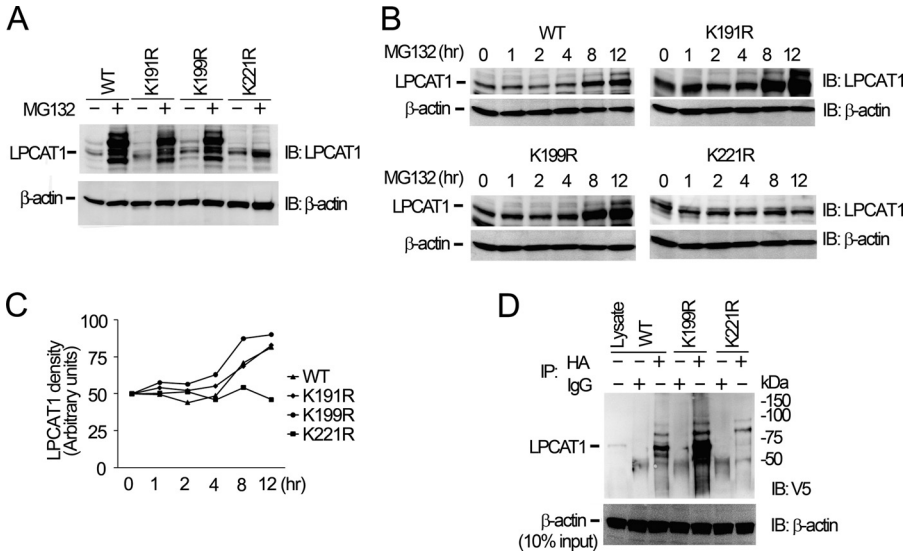

FIGURE 5. **Lys^{221} within LPCAT1 is a ubiquitin acceptor site for SCF$^{\beta\text{-TrCP}}$.** *A,* MLE cells were nucleofected with wild type and lysine-mutated LPCAT1 plasmids for 16 h followed by MG132 treatment for another 12 h. Cell lysates were analyzed by immunoblotting (*IB*). *B* and *C,* nucleofected cells were treated with MG132 in a time course, and cell lysates were subjected to LPCAT1 immunoblotting (*B*), and the densitometry of the immunoblotting results was plotted (*C*). *D,* HA-tagged β-TrCP and V5-tagged wild type or lysine-mutated LPCAT1 plasmids were co-expressed in cells, and HA immunoprecipitation (*IP*) was performed followed by V5 immunoblotting. Each panel is representative of three independent experiments except *D* ($n = 2$).

Lys^{221} is a critical residue for site-specific LPCAT1 polyubiquitination.

LPS Induces LPCAT1 Degradation by a β-TrCP-GSK-3β Mechanism—As surfactant phospholipid biosynthesis is reduced during Gram-negative sepsis (18), we hypothesized that LPCAT1 life span would be reduced after exposure to lipopolysaccharide. Indeed, LPS reduced immunoreactive LPCAT1 levels in a concentration-dependent (5–20 μg/ml, see Fig. 6*A*) and time-dependent (18–24 h, Fig. 6*B*) manner, an effect that was blocked with MG132 treatment. When cells were exposed to LPS or cycloheximide and then silenced using β-TrCP siRNA, LPCAT1 levels were restored as compared with cells exposed to LPS or protein synthesis inhibitor alone (Fig. 6*C*). LPS activates GSK-3β (19). GSK-3β knockdown by siRNA also restored immunoreactive LPCAT1 levels after cycloheximide or LPS treatment (Fig. 6*D*). These data suggest that LPCAT1 is pathophysiologically regulated and implicate a β-TrCP-GSK-3β pathway as a potentially important effector mechanism in LPS-induced LPCAT1 degradation.

To extend the above observations to a sepsis model *in vivo*, we assessed the major airway-secreted product of LPCAT1, surfactant PtdCho, and measured surfactant lung biophysical properties (Fig. 7). Mice were given diluent, infected with a lentiviral vector alone, or lentivirus encoding LPCAT1 for 96 h prior exposure to LPS for 24 h. In mice given LPS, immunoblotting revealed that LPCAT1 was significantly decreased in lungs compared with untreated mice as revealed by densitometry ($p = 0.02$, $n = 12$) (Fig. 7*A*, *upper row*). Importantly, LPCAT1 gene transfer significantly increased immunoreactive LPCAT1 content and partially restored these levels in mice given LPS (Fig. 7*A*, *lower row*). LPS significantly impaired respiratory mechanics as it increased airway resistance and elastance (lung stiffness) (Fig. 7, *B* and *D*), reduced compliance (Fig. 7*C*), and markedly reduced surfactant phospholipid levels (Fig. 7*F*). LPCAT1 lentiviral gene transfer partially

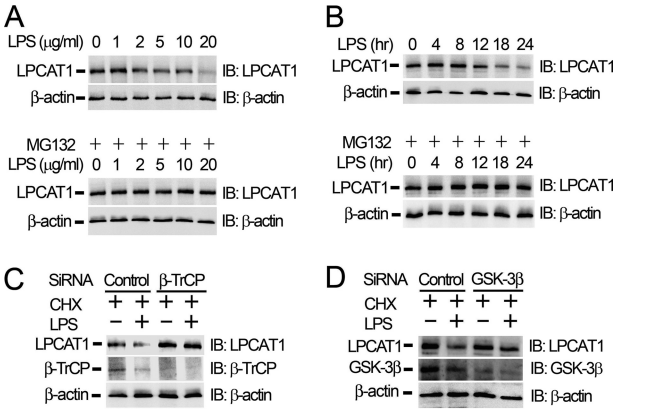

FIGURE 6. **LPS triggers LPCAT1 degradation via the ubiquitin proteasome.** *A,* MLE cells were maintained in serum-free medium and exposed to different concentrations of LPS in the presence or absence of MG132 for 24 h. Cell lysates were analyzed by LPCAT1 and β-actin immunoblotting (*IB*). *B,* cells were exposed to LPS (10 μg/ml) in the presence or absence of MG132, and cells were collected in a time course for LPCAT1 immunoblotting. *C* and *D,* cells were transfected with control RNA, β-TrCP siRNA, or GSK-3β siRNA oligos for 48 h followed by treatment with cycloheximide (*CHX*) (10 μg/ml) with or without LPS (10 μg/ml) for another 12 h as indicated. Cell lysates were processed for LPCAT1, β-TrCP, or GSK-3β immunoblotting. Each panel is representative of three independent experiments.

reversed these adverse effects on lung mechanics in mice (Fig. 7, *B–E*) that was due, in part, to increased surfactant levels (Fig. 7*F*). Thus, LPS destabilizes LPCAT1 *in vivo* leading to reduced surfactant lipid and impaired lung functional properties that can be lessened with gene transfer of the phospholipid remodeling enzyme.

DISCUSSION

A unique feature of distal lung (type II) epithelia is that they have a highly differentiated lipogenic phenotype characterized by the ability to rapidly synthesize DPPtdCho, a saturated phospholipid that is secreted into airways into the surfactant film to lower alveolar surface tension to maintain lung stabil-

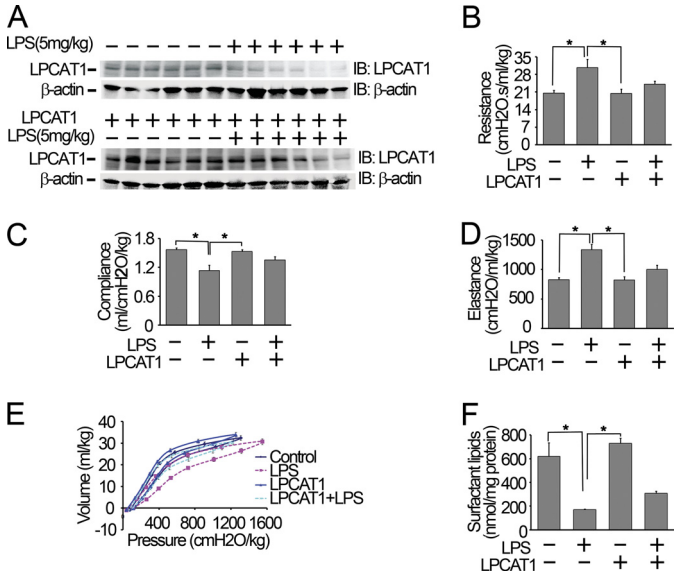

FIGURE 7. **LPS down-regulates LPCAT1 in a mouse model.** *A–F,* mice were given vector alone or a lentivirus encoding LPCAT1 (10^8 plaque-forming units/mouse) for 96 h prior to intratracheal inoculation with LPS (5 mg/kg) for 24 h. Animals were then mechanically ventilated, and lung resistance (*B*), compliance (*C*), and elastance (lung stiffness, *D*) were measured and pressure-volume loops (*E*) generated. Each group contained 4–6 mice. Mice lung tissues were also homogenized and sonicated in cell lysis buffer followed by LPCAT1 immunoblotting (*IB*) analysis (*A*). *, $p < 0.05$ *versus* groups as indicated by analysis of variance. *F,* PtdCho levels in lung lavage were assayed in groups.

ity. It has been estimated that ~55–75% of surfactant DPPtdCho is synthesized by the remodeling pathway, via LPCAT1, with the remainder generated by *de novo* synthesis (1–3). The recent identification and enzymatic characterization of LPCAT1 underscore its pivotal role in maintenance of the surfactant phenotype, and yet its molecular behavior requires investigation. Here, we show that LPCAT1 is a phosphoenzyme regulated at the level of protein stability. Phosphorylation of Ser^{178} and Ser^{182} within a phosphodegron by GSK-3β then primes LPCAT1 for subsequent polyubiquitination by the $SCF^{\beta\text{-TrCP}}$ complex leading to its disposal by the proteasome. This pathway appears to be physiologically relevant during septic lung injury, as LPS was highly effective in decreasing immunoreactive LPCAT1 and PtdCho levels. Although speculative, the data suggest that future studies using small molecule $SCF^{\beta\text{-TrCP}}$ complex antagonists might be a strategy to enhance LPCAT1 life span during pulmonary sepsis to preserve surfactant levels and maintain lung function.

Mammalian cells typically eliminate lipogenic proteins using lysosomal or proteasomal mechanisms. Here, turnover of native LPCAT1 protein levels was relatively rapid compared with other lipogenic substrates (18, 22). Unlike our findings with CTP:phosphocholine cytidylyltransferase, an indispensable enzyme involved in *de novo* PtdCho synthesis that is degraded by the lysosome (16), LPCAT1 processing occurs via ubiquitin-proteasome-mediated degradation. Inhibition of protein synthesis by cycloheximide showed that LPCAT1 protein $t_{1/2}$ is ~4 h, but the enzyme is likely destabilized very rapidly in cells after endotoxin exposure. These results are in line with our recent observations that bacterial pathogens involved in severe infection exploit the proteolytic (ubiquitin) machinery as a means to eliminate key lipogenic proteins to accentuate injury in the host (17).

Of the F-box subunits tested, only $SCF^{\beta\text{-TrCP}}$ was observed to ubiquitinate LPCAT1. $SCF^{\beta\text{-TrCP}}$ ubiquitin E3 ligase is critical in promoting cell cycle progression, and the complex exhibits oncogenic properties (10). The ability of β-TrCP to target LPCAT1 for ubiquitination is highly compatible with the pro-oncogenic behavior of $SCF^{\beta\text{-TrCP}}$ given that LPCAT1 may be viewed as a marker of cell differentiation (4, 6, 7). As alveolar cells transition from synthesizing DPPtdCho for airway secretion to production of unsaturated PtdCho destined for new cell membrane formation, it is possible that $SCF^{\beta\text{-TrCP}}$ modulates the alveolar cell phenotype by limiting LPCAT1 availability; in this way, the cell might redirect phospholipid synthesis toward generating unsaturated PtdCho molecular species needed for cell proliferation commensurate with its oncogenic characteristics (10). $SCF^{\beta\text{-TrCP}}$ recognizes a DSG*XXS* destruction motif, and variants (DS(G/D)D(G/E)E(G/S)S*GXX*(S/E/D)) have been amply demonstrated (10). The minimal destruction motif for β-TrCP recognition within LPCAT1, ^{178}SDQDS^{182}, represents a modified and somewhat unique molecular signature similar to the phosphatase, CDC25A, that regulates cyclin-dependent kinases (23). This LPCAT1 signature is both required and sufficient for $SCF^{\beta\text{-TrCP}}$ recognition.

The SCF^{TrCP} E3 complex binds to substrate phosphodegrons after Ser/Thr residues have been phosphorylated. Data base analysis of the LPCAT1 primary sequence using a phosphorylation prediction tool identified two potential sites for GSK-3β phosphorylation, Ser^{178} (^{178}SDQDSRRKT) and Ser^{518} (^{518}SPENS). When integrating the adjacent amino acid composition of these two putative molecular sites with the tandem structure of Ser/Thr clustering, Ser^{178} was an attractive candidate for GSK-3β phosphorylation. Of note, although GSK-3β phosphorylated wild type LPCAT1 *in vitro*, LPCAT1 double or point mutants at S178A or S182A were significantly less prone to *in vivo* phosphorylation, displayed limited ability to bind GSK-3β or SCF^{TrCP}, and did not accumulate in the presence of MG132. Other loss-of-function and gain-of function studies demonstrated that GSK-3β regulates LPCAT1 protein abundance. Gene silencing of GSK-3β, also effectively rescues LPS-induced LPCAT1 degradation. Collectively, these results implicate GSK-3β as an *in vivo* regulator for LPCAT1 site-specific phosphorylation-dependent proteolysis.

LPCAT1 harbors a consensus sequence for GSK-3β phosphorylation, with tandem repeats of this consensus motif that may drive progressive phosphorylation (24). Primed phosphorylation of SDQDS within LPCAT1 at the C-terminal Ser (Ser^{182}) in concert with GSK-3β-catalyzed phosphorylation at the N-terminal Ser (S^{178}) may represent a mechanism for $SCF^{\beta\text{-TrCP}}$ docking. This mechanism is supported by lack of ability of GSK-3β to phosphorylate either Ser point mutant (Fig. 4*C*). Specifically, the dependence of Ser^{178} for priming by Ser^{182} phosphorylation is evidenced by lack of an intense phosphorylation signal detected in our autoradiograms after GSK-3β incubation with the S182A LPCAT1 mutant that may impinge on GSK-3β docking near the acceptor site (Ser^{178}). Although the identity of the initiator kinase remains

unknown, preliminary knockdown of PKC-β attenuates LPCAT1 degradation making PKC-β a candidate interactor especially given its role in priming other substrates such as insulin receptor substrate-1 (25). In the process of manuscript preparation, Morimoto *et al.* (26) demonstrated that a related isoform, lysophosphatidylcholine acyltransferase-2 (LPCAT2), undergoes site-specific phosphorylation (Ser^{34}) and enzyme activation by MAPKs via an LPS-Toll receptor pathway. LPCAT2 is involved in the generation of the proinflammatory phospholipid, platelet-activating factor. These results are intriguing as they suggest that LPCAT1 might also harbor upstream phosphoacceptor sites that differentially regulate its enzymatic behavior after endotoxin. Interestingly, another recent study showed that a mutation in exon 3 of the *Lpcat1* gene leads to generation of an LPCAT1 variant linked to reduced DPPtdCho and photoreceptor dysfunction in the retina (27). Because this LPCAT1 variant is nonfunctional and truncated (with a stop after residue 178, size ~20 kDa), it also is likely eliminated but by unknown mechanisms given that it lacks the ubiquitin acceptor site.

Although we have characterized destabilizing elements within the LPCAT1 primary sequence, proteins may contain additional motifs, structural features, or interact with second messengers or ligands that can, under certain circumstances, alter protein half-life. Calmodulin, a calcium sensor, binds and stabilizes the monoubiquitinated enzyme CTP:phosphocholine cytidylyltransferase and antagonizes actions of a calcium-activated neutral proteinase, calpain (16, 28). LPCAT1 is a calcium-binding protein that harbors two calcium-binding (EF hand) motifs that reside within the C-terminal enzyme. Exogenous calcium triggers LPCAT1 nuclear import, and deletion of these two EF hand motifs stabilizes the LPCAT1 protein,[3] suggesting that calcium might play an important role in signaling LPCAT1 degradation. It is possible that LPCAT1 interacts with calcium via EF hand domains in concert with other known calcium adaptors (*e.g.* calmodulin or calmodulin kinase). If confirmed, this mechanism would add another level of complexity to LPCAT1 proteolytic processing that either facilitates or modifies $SCF^{\beta TrCP}$-dependent ubiquitination of this substrate. Studies investigating the underlying molecular mechanisms of EF-hand motifs in LPCAT1 protein turnover are ongoing.

[3] C. Zou and R. K. Mallampalli, unpublished data.

REFERENCES

1. den Breejen, J. N., Batenburg, J. J., and van Golde, L. M. (1989) *Biochim. Biophys. Acta* **1002,** 277–282
2. Post, M., Schuurmans, E. A., Batenburg, J. J., and Van Golde, L. M. (1983) *Biochim. Biophys. Acta* **750,** 68–77
3. Mason, R. J., and Dobbs, L. G. (1980) *J. Biol. Chem.* **255,** 5101–5107
4. Chen, X., Hyatt, B. A., Mucenski, M. L., Mason, R. J., and Shannon, J. M. (2006) *Proc. Natl. Acad. Sci. U.S.A.* **103,** 11724–11729
5. Nakanishi, H., Shindou, H., Hishikawa, D., Harayama, T., Ogasawara, R., Suwabe, A., Taguchi, R., and Shimizu, T. (2006) *J. Biol. Chem.* **281,** 20140–20147
6. Bridges, J. P., Ikegami, M., Brilli, L. L., Chen, X., Mason, R. J., and Shannon, J. M. (2010) *J. Clin. Invest.* **120,** 1736–1748
7. Butler, P. L., and Mallampalli, R. K. (2010) *J. Biol. Chem.* **285,** 6246–6258
8. d'Azzo, A., Bongiovanni, A., and Nastasi, T. (2005) *Traffic* **6,** 429–441
9. Cardozo, T., and Pagano, M. (2004) *Nat. Rev. Mol. Cell Biol.* **5,** 739–751
10. Frescas, D., and Pagano, M. (2008) *Nat. Rev. Cancer* **8,** 438–449
11. Wang, C. Y., Lin, Y. S., Su, W. C., Chen, C. L., and Lin, C. F. (2009) *Mol. Biol. Cell.* **20,** 4153–4161
12. Tachado, S. D., Li, X., Swan, K., Patel, N., and Koziel, H. (2008) *J. Biol. Chem.* **283,** 33191–33198
13. Xu, C., Kim, N. G., and Gumbiner, B. M. (2009) *Cell Cycle* **8,** 4032–4039
14. Sundqvist, A., Bengoechea-Alonso, M. T., Ye, X., Lukiyanchuk, V., Jin, J., Harper, J. W., and Ericsson, J. (2005) *Cell Metab.* **1,** 379–391
15. Filali, M., Cheng, N., Abbott, D., Leontiev, V., and Engelhardt, J. F. (2002) *J. Biol. Chem.* **277,** 33398–33410
16. Chen, B. B., and Mallampalli, R. K. (2009) *Mol. Cell. Biol.* **29,** 3062–3075
17. Ray, N. B., Durairaj, L., Chen, B. B., McVerry, B. J., Ryan, A. J., Donahoe, M., Waltenbaugh, A. K., O'Donnell, C. P., Henderson, F. C., Etscheidt, C. A., McCoy, D. M., Agassandian, M., Hayes-Rowan, E. C., Coon, T. A., Butler, P. L., Gakhar, L., Mathur, S. N., Sieren, J. C., Tyurina, Y. Y., Kagan, V. E., McLennan, G., and Mallampalli, R. K. (2010) *Nat. Med.* **16,** 1120–1127
18. Mallampalli, R. K., Ryan, A. J., Salome, R. G., and Jackowski, S. (2000) *J. Biol. Chem.* **275,** 9699–9708
19. Huang, W. C., Lin, Y. S., Wang, C. Y., Tsai, C. C., Tseng, H. C., Chen, C. L., Lu, P. J., Chen, P. S., Qian, L., Hong, J. S., and Lin, C. F. (2009) *Immunology* **128,** e275–e286
20. Deleted in proof
21. Deleted in proof
22. Hargrove, J. L., and Schmidt, F. H. (1989) *FASEB J.* **3,** 2360–2370
23. Busino, L., Donzelli, M., Chiesa, M., Guardavaccaro, D., Ganoth, D., Dorrello, N. V., Hershko, A., Pagano, M., and Draetta, G. F. (2003) *Nature* **426,** 87–91
24. Zhou, B. P., Deng, J., Xia, W., Xu, J., Li, Y. M., Gunduz, M., and Hung, M. C. (2004) *Nat. Cell Biol.* **6,** 931–940
25. Liberman, Z., Plotkin, B., Tennenbaum, T., and Eldar-Finkelman, H. (2008) *Am. J. Physiol. Endocrinol. Metab.* **294,** E1169–E1177
26. Morimoto, R., Shindou, H., Oda, Y., and Shimizu, T. (2010) *J. Biol. Chem.* **285,** 29857–29862
27. Friedman, J. S., Chang, B., Krauth, D. S., Lopez, I., Waseem, N. H., Hurd, R. E., Feathers, K. L., Branham, K. E., Shaw, M., Thomas, G. E., Brooks, M. J., Liu, C., Bakeri, H. A., Campos, M. M., Maubaret, C., Webster, A. R., Rodriguez, I. R., Thompson, D. A., Bhattacharya, S. S., Koenekoop, R. K., Heckenlively, J. R., and Swaroop, A. (2010) *Proc. Natl. Acad. Sci. U.S.A.* **107,** 15523–15528
28. Chen, B. B., and Mallampalli, R. K. (2007) *J. Biol. Chem.* **282,** 33494–33506